Tectonic approach for waste-to-nanomaterial transformation towards polyethylene recycling

Yanan Huang,[a] *Chi-Linh Do-Thanh,*[b] *Zhenzhen Yang,*[*c] *Sheng Dai,*[*b,c] *Hao Chen,*[*a,b]

[a] State Key Laboratory for Chemo and Biosensing, College of Chemistry and Chemical Engineering, Hunan University, Changsha, 410082, China.

[b] Department of Chemistry, Institute for Advanced Materials and Manufacturing, University of Tennessee, Knoxville, TN 37996, USA.

[c] Chemical Sciences Division, Oak Ridge National Laboratory, Oak Ridge, TN 37831, USA.

* Corresponding author.

E-mail address: chenhaoch@hnu.edu.cn (H. Chen), yangz3@ornl.gov (Z. Yang), dais@ornl.gov (S. Dai)

Table of contents

Materials

All reagents and solvents [Polyethylene (M=3000, 35000; Aldrich, USA), Sodium amide ($NaNH_2$, AR, Fisher Scientific, USA)] were purchased from commercial sources and were used without further purification, unless indicated otherwise.

Characterization

The powder X-ray diffraction (PXRD) data were recorded with a PANalytical Empyrean diffractometer, operated at 45 kV and 40 mA (scanning step: 0.02° per step). The diffraction patterns were recorded in the range of 5-60°. $\lambda = 0.1540598$ nm. Field emission scanning electron microscopy (SEM) observations were performed on a Hitachi S-4800 microscope operated at an accelerating voltage of 15.0 kV. Transmission electron microscopy (TEM) were conducted on an aberration-corrected FEI Titan S 80-300. FTIR spectra of the samples were collected on a TENSOR 27 FTIR at a resolution of 2 cm^{-1}. X-ray photoelectron spectroscopy (XPS) was performed with a Thermo Scientific Model K-Alpha XPS Instrument. The instrument uses micro-focused, monochromatic Al Kα X-rays (1486.6 eV). The X-ray spot can be focused to a range of spot sizes from 30 to 400 microns. Thermogravimetric analyses (TGA) were performed under air on a SII Nanotechnology TGA 2950, with a heating rate of 10 °C mim^{-1}. The nitrogen adsorption and desorption isotherms were measured at 77 K under a Gemini 2360 surface area analyzer. The samples were outgassed at 150 °C for 16 h before the measurements. Surface areas were calculated from the adsorption data using Brunauer–Emmett–Teller (BET) methods. The pore-size-distribution curves were obtained from the adsorption branches using non-local density functional theory (NLDFT) method. The CO_2 adsorption and desorption isotherms were measured at 273 and 298 K by Autosorb-1-C Quantachrome analyzer. Elemental analyses were performed by Atlantic Microlab Inc., Norcross, GA.

Synthesis procedure

A mixture composed of $NaNH_2$ (0.1–0.75 g) and polyethylene (1 g) was placed in a nickel crucible and then heated in a tubular furnace under flowing N_2 (100 mL/min) to a target temperature of 500 °C with ramping rate of 5 °C/min, keeping the temperature for 1 h, and then further increased to 650–850 °C, keeping for 2 h (The corresponding molar ratios of $NaNH_2$ to the $–CH_2–CH_2–$ repeat unit were calculated to be 0.072, 0.18, 0.36, and 0.54 for $NaNH_2$ loadings of 0.10, 0.25, 0.50, and 0.75 g per 1 g of PE, respectively). The resultant powder was washed with deionized water to neutral, followed by being dried at 120 °C for 12 h. The obtained carbon was named as C-M-N, (M refers to the ratio of $NaNH_2$/Polyethylene, N refers to the heating temperature). Yield of carbon = (Mass of carbon obtained)/(Mass of polyethylene in the starting material).

Calculation of CO_2/N_2 selectivity

The isotherm data for CO_2 and N_2 were fitted with the dual-site Langmuir-Freundlich model as follows.

$$q = q_{A,sat}\frac{b_A p^{v_A}}{1+b_A p} + q_{B,sat}\frac{b_B p^{v_B}}{1+b_B p}$$

where p is the pressure of the bulk gas at equilibrium with the adsorbed phase (kPa), q is the adsorbed amount per mass of adsorbent (mol kg^{-1}), $q_{A,sat}$ an $q_{B,sat}$ are the saturation capacities of site A and B (mmol g^{-1}), b_A and b_B are the affinity coefficients (kPa^{-1}), v_A and v_B represent the deviations from an ideal homogeneous surface.

Calculation of Q_{st}

The isosteric heats of adsorption (Q_{st}) was used to explore the binging energy of C_3H_4, which is defined as follows,

$$Q_{st} = -R\sum_{i=0}^{m} a_i N^i$$

The calculations were based on the Virial equations fitted by isotherms of two different temperatures (298 and 273 K).

$$\ln p = \ln N + \frac{1}{T}\sum_{i=0}^{m} a_i N^i + \sum_{i=0}^{m} b_i N^i$$

where p (bar) is the pressure of the bulk gas at equilibrium with the adsorbed phase, N (mmol g^{-1}) is the adsorbed amount per mass of adsorbent, T (K) is the test temperature, while a_i (i=1-5) and b_i (i=1-3) are the Virial constants.

CV measurement

A three-electrode system was used to evaluate the capacitive performance of the as-prepared porous carbons by $NaNH_2$-promoted cross-linking/carbonization on a CHI 760C electrochemical workstation (Shanghai ChenHua Instruments Co., China). The test was performed in 1M H_2SO_4 aqueous solution with a platinum foil and Ag/AgCl (1 M KCl) as the counter electrode and reference electrode, respectively. The working electrodes were prepared by casting the 10 μL sample ink onto a glass carbon electrode and the sample ink was prepared by 14 mg carbon samples, 4 mg carbon black, 1mL isopropanol with 40 μL Nafion solution (5%) as binder with the aid of sonification for 1 hour. The capacitive performance of samples was studied by using cyclic voltammetry (CV), galvanostatic charge–discharge (GCD) in the voltage range of −0.2 V–0.8 V to avoid H_2O decomposition. The gravimetric capacitances (C, F/g) based on CV curves and GCD curves were calculated from Equation (1) and Equation (2), respectively.

$$(1)\ C = \frac{\int_{-0.2}^{0.8} I(V)dV}{2mVS};(2)\ C = \frac{It}{mV}$$

Where I is the discharge current (A), m is the mass of electrode active materials (g), S is the scan rate (V/s), V is the voltage window (V) and t is the discharging time (s).

Supplementary figures and tables

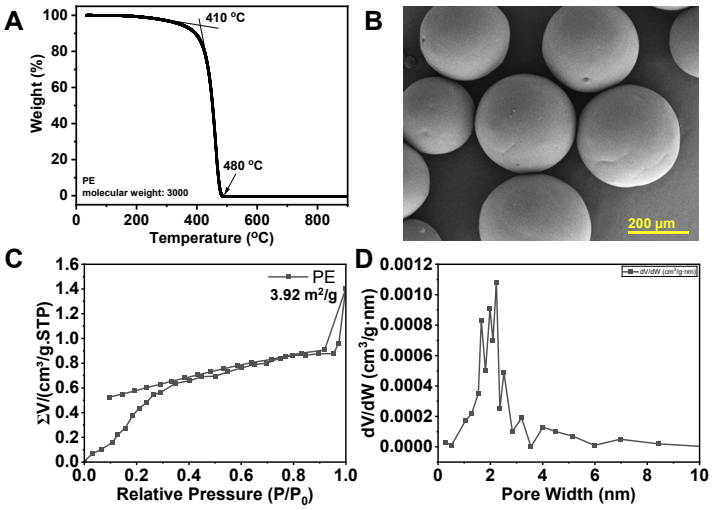

Figure S1 (A) Thermogravimetric analysis (TGA) result of PE precursor (molecular weight: 3000) obtained under N_2 atmosphere with a ramping rate of 10 °C min^{-1}. (B) SEM images showing the morphology of the PE precursor. (C) N_2 adsorption–desorption isotherms of the PE precursor. (D) Pore size distribution of the PE precursor derived from the adsorption data.

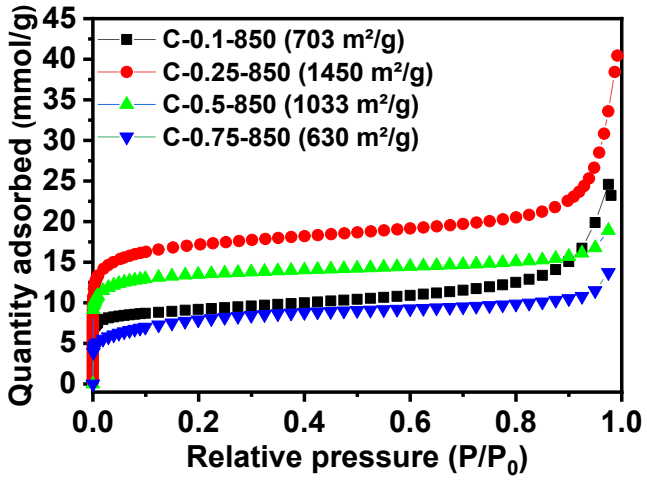

Figure S2 N_2 isotherms (77K) of the carbon materials obtained at 850 °C with different mass ratio of $NaNH_2$:PE.

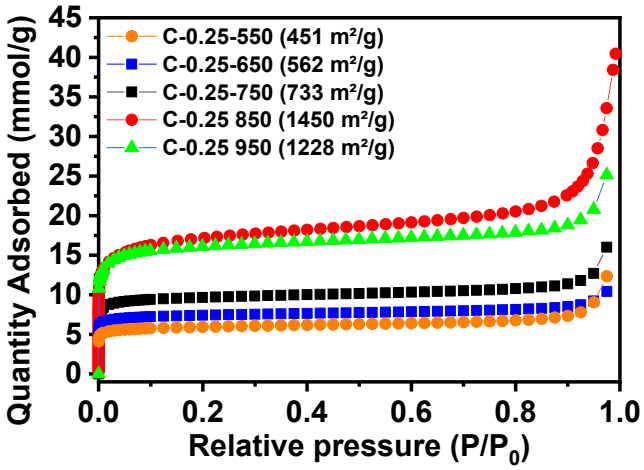

Figure S3 N_2 isotherms (77K) of the carbon materials obtained at the $NaNH_2$:PE mass ratio of 0.25 and different reaction temperatures.

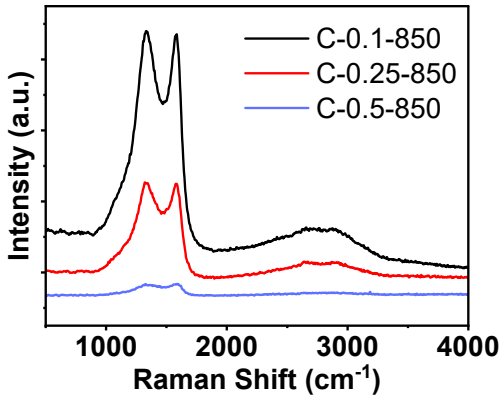

Figure S4 Raman spectra of C-0.1-850, C-02.5-850 and C-0.5-850.

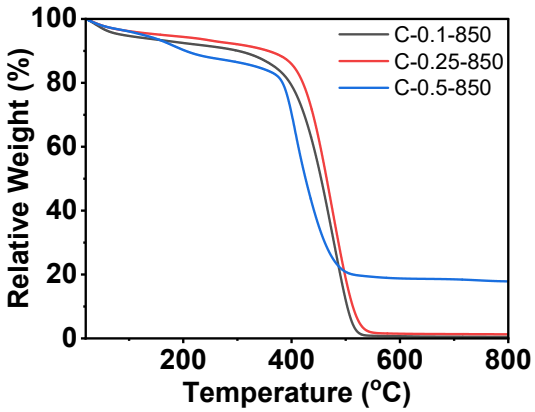

Figure S5 TGA analysis of C-0.1-850, C-02.5-850 and C-0.5-850.

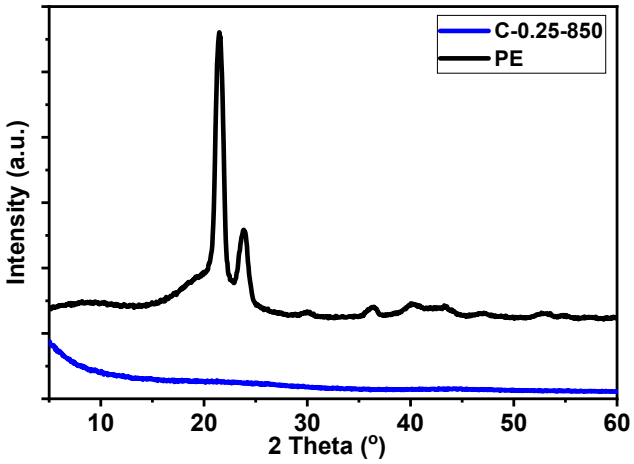

Figure S6 PXRD pattern of the PE precursor and the C-0.25-850 obtained with a $NaNH_2$:PE mass ratio of 0.25 and reaction temperature of 850 °C.

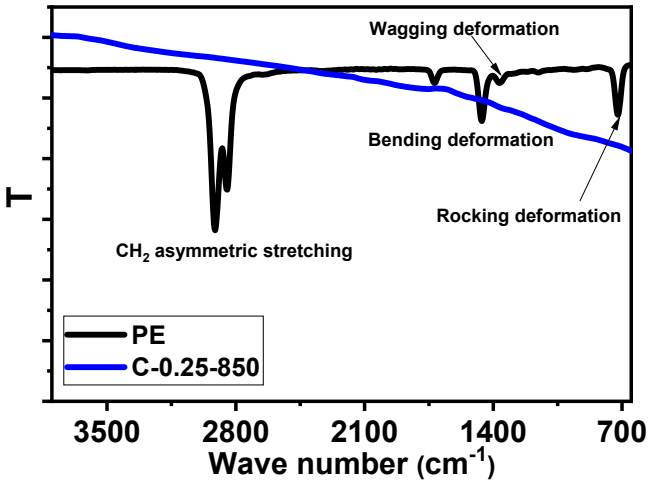

Figure S7 FTIR spectra of the PE precursor and the C-0.25-850 obtained with a $NaNH_2$:PE mass ratio of 0.25 and reaction temperature of 850 °C.

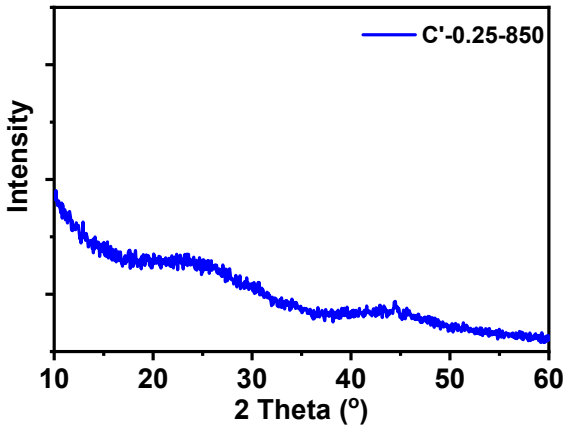

Figure S8 PXRD pattern of C'-0.25-850 obtained with a $NaNH_2$:PE35000 mass ratio of 0.25 and reaction temperature of 850 °C.

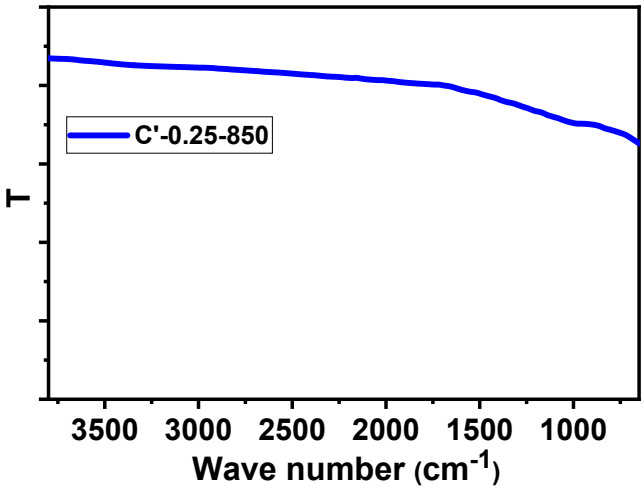

Figure S9 FTIR spectrum of C'-0.25-850 obtained with a $NaNH_2$:PE35000 mass ratio of 0.25 and reaction temperature of 850 °C.

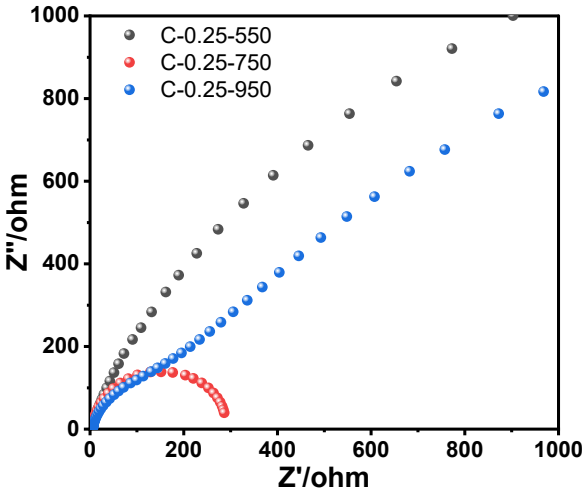

Figure S10. EIS measurements of C-0.25-550, C-0.25-750, and C-0.25-950.

Table S1 surface area of the carbon materials fabricated in this work and previous literature using PE as the precursor.

Carbon materials	Catalyst/activator	Temperature [^{o}C]	Surface area [m^2 g^{-1}]	Ref.
C-0.25-850	$NaNH_2$	850	1450	This work
C'-0.25-850	$NaNH_2$	850	2080	This work
PE-PC	MCHP [a]	900	255	[1]
PE-HPC	MCHP [a]	900	767	[1]
PE-HPC-800NH_3	MCHP [a] -NH_3	900-800	1117	[1]
PE-HPC-900NH_3	MCHP [a] -NH_3	900-900	1219	[1]
PE-HPC-1000NH_3	MCHP [a] -NH_3	900-1000	1012	[1]
CNT	$Co(NO_3)_2$	500	195.7	[2]

[a] MCHP was $4MgCO_3 \cdot Mg(OH)_2 \cdot 5H_2O$.

Table S2 CO_2 uptake performance of the carbons derived from PE and data from the literature.

Carbon materials	Surface area [m^2 g^{-1}]	CO_2 uptake capacity [mmol g^{-1}]		Reference
		273 K, 1 bar	298 K, 1 bar	
C-0.1-850	703	5.15	3.53	This work
C-0.25-850	1450	5.31	3.31	This work
C-0.5-850	1033	4.54	3.05	This work
C-0.75-850	630	1.78	1.15	This work
C-0.25-550	450	3.29	2.61	This work
C-0.25-650	562	3.43	2.76	This work
C-0.25-750	733	5.15	3.75	This work
C-0.25-950	1228	4.89	3.71	This work
C'-0.25-850	2080	5.21	3.53	This work
MC600	479	~2.0	~1.3	[3]
NMC600-330-1h	907	3.97	~2.6	[3]
CBAP-1	865	3.20	2.20	[4]
c-CBAP-1N	1063	5.09	3.50	[4]
Palm kernel shell	367.8		2.13	[5]
Norit® SX2	660.7		1.88	[5]
PAC2	167.08		1.66 (303K)	[6]
TC-EMC	3840		3.2	[7]
N-TC-EMC	2559		4.00	[7]
N-TC-Y1	1762		3.20	[7]
GSK0.5-700	1714	4.74	3.28	[8]
SK-700	714	3.02	2.81	[8]
HMT-80-1000	936	5.50	4.00	[9]
MCN/C	338	3.05	2.35	[10]
HCM_DAH-1	670	3.30	2.60	[11]
HCM-DAH-1-900-3	1392	4.90	3.30	[11]
H-NMC-2.5[a]	537		2.80	[12]
RFL-500[a]	467		3.1	[13]
NMC-His-700[a]	1114	3.30	~1.80	[14]
NMC-His-900[a]	1225	3.60	~2.20	[14]
NOMC-800[a]	631	3.20	2.90	[15]

NOMC-800-K[a]	1413	4.60	3.10	[15]
CMC-1[a]	1082	4.80	3.20	[16]
CMC-2[a]	1994	4.84	3.08	[16]
CMC-3[a]	1405	6.27	5.22	[16]
CK-600-3[a]	1383	6.00	4.0	[17]
NGC-650-4[a]	1824	6.23	3.92	[18]

[a] Nitrogen-doped carbon.

Reference

1 Y. Lian; M. Ni; Z. Huang; R. Chen; L. Zhou; W. Utetiwabo; W. Yang. *Chem Eng J* 2019, **366**, 313-320.
2 Z. Huang; Y. Zheng; H. Zhang; F. Li; Y. Zeng; Q. Jia; J. Zhang; J. Li; S. Zhang. *J Mater Sci Technol* 2021, **94**, 90-98.
3 K. Huang; S.-H. Chai; R. T. Mayes; G. M. Veith; K. L. Browning; M. A. Sakwa-Novak; M. E. Potter; C. W. Jones; Y.-T. Wu; S. Dai. *Chem Commun* 2015, **51** (97), 17261-17264.
4 P. Puthiaraj; Y.-R. Lee; W.-S. Ahn. *Chem Eng J* 2017, **319**, 65-74.
5 N. A. Rashidi; S. Yusup. *Journal of Cleaner Production* 2017, **168**, 474-486.
6 N. S. Nasri; U. D. Hamza; S. N. Ismail; M. M. Ahmed; R. Mohsin. *Journal of Cleaner Production* 2014, **71**, 148-157.
7 L. Wang; R. T. Yang. *The Journal of Physical Chemistry C* 2012, **116** (1), 1099-1106.
8 A. Alabadi; S. Razzaque; Y. Yang; S. Chen; B. Tan. *Chem Eng J* 2015, **281**, 606-612.
9 L. Liu; Q.-F. Deng; X.-X. Hou; Z.-Y. Yuan. *J Mater Chem* 2012, **22** (31), 15540-15548.
10 Q.-F. Deng; L. Liu; X.-Z. Lin; G. Du; Y. Liu; Z.-Y. Yuan. *Chem Eng J* 2012, **203**, 63-70.
11 G.-P. Hao; W.-C. Li; D. Qian; G.-H. Wang; W.-P. Zhang; T. Zhang; A.-Q. Wang; F. Schüth; H.-J. Bongard; A.-H. Lu. *J Am Chem Soc* 2011, **133** (29), 11378-11388.
12 J. Wei; D. Zhou; Z. Sun; Y. Deng; Y. Xia; D. Zhao. *Adv Funct Mater* 2013, **23** (18), 2322-2328.
13 G. P. Hao; W. C. Li; D. Qian; A. H. Lu. *Adv Mater* 2010, **22** (7), 853-857.
14 X. Gao; Z. Chen; Y. Yao; M. Zhou; Y. Liu; J. Wang; W. D. Wu; X. D. Chen; Z. Wu; D. Zhao. *Adv Funct Mater* 2016, **26** (36), 6649-6661.
15 J. Yu; M. Guo; F. Muhammad; A. Wang; G. Yu; H. Ma; G. Zhu. *Micropor Mesopor Mater* 2014, **190**, 117-127.
16 Y. Boyjoo; Y. Cheng; H. Zhong; H. Tian; J. Pan; V. K. Pareek; J.-F. Lamonier; M. Jaroniec; J. Liu. *Carbon* 2017, **116**, 490-499.
17 L. Yue; Q. Xia; L. Wang; L. Wang; H. DaCosta; J. Yang; X. Hu. *J Colloid Interface Sci* 2018, **511**, 259-267.
18 L. Yue; L. Rao; L. Wang; L. An; C. Hou; C. Ma; H. DaCosta; X. Hu. *Energ Fuel* 2018, **32** (6), 6955-6963.